

Supplementary Information

Heteropoly Acid Functionalized Fluoroelastomer with Outstanding Chemical Durability and Performance for Vehicular Fuel Cells

Andrew R. Motz,^a Mei-Chen Kuo,^a James L. Horan,^a Rameshwar Yadav,^b Soenke Seifert,^c Tara P. Pandey,^a Samuel Galioto,^a Yuan Yang,^d Nilesh V. Dale,^b Steven J. Hamrock,^e and Andrew M. Herring,^{a*}

^aDepartment of Chemical and Biological Engineering, Colorado School of Mines, Golden, Colorado 80401, USA. E-mail: aherring@mines.edu

^bNissan Technical Center North America, Farmington Hills, Michigan 48331, USA

^cX-ray Science Division, Advanced Photon Source, Argonne National Laboratory, Argonne, IL 60439, USA

^dDepartment of Chemistry and Geochemistry, Colorado School of Mines, Golden, Colorado 80401, USA

^eEnergy Components Program, 3M, St. Paul, MN 55144, USA

* To whom correspondence should be addressed (A. Herring):

Colorado School of Mines, Golden, Colorado 80401, USA.

E-mail: aherring@mines.edu

Supporting Information

Synthesis of PolyHPA:

IR spectra for species involved in the functionalization of FC-2178 to form PolyPPA can be seen in Figure S1a. The IR spectra are dominated by the $-\text{CF}_2-$ stretching bands at 1200 and 1130 cm^{-1} (symmetric and asymmetric, respectively) for FC-2178 and the PolyPPA.¹ Strong bands from the aromatic group at 1200 and 1180 cm^{-1} are present in both the DHPP and the PolyPPA, as expected. While the C-O-Ar bond formed in step 1 is not identified, the washed functionalized PolyPPA shows signatures of aromatic groups, which would have washed away if not covalently attached to the polymer. The next step in the synthesis is attaching HSiW11 to the PolyPPA. The reactants and product for the attachment of HSiW11 to PolyPPA are displayed in Figure S1b. It is evident that signatures from both HSiW11 and PolyPPA exist in the washed PolyHPA. Most notably are the $-\text{CF}_2-$ stretching bands and the strong W-O bands between 700 and 1000 cm^{-1} .²

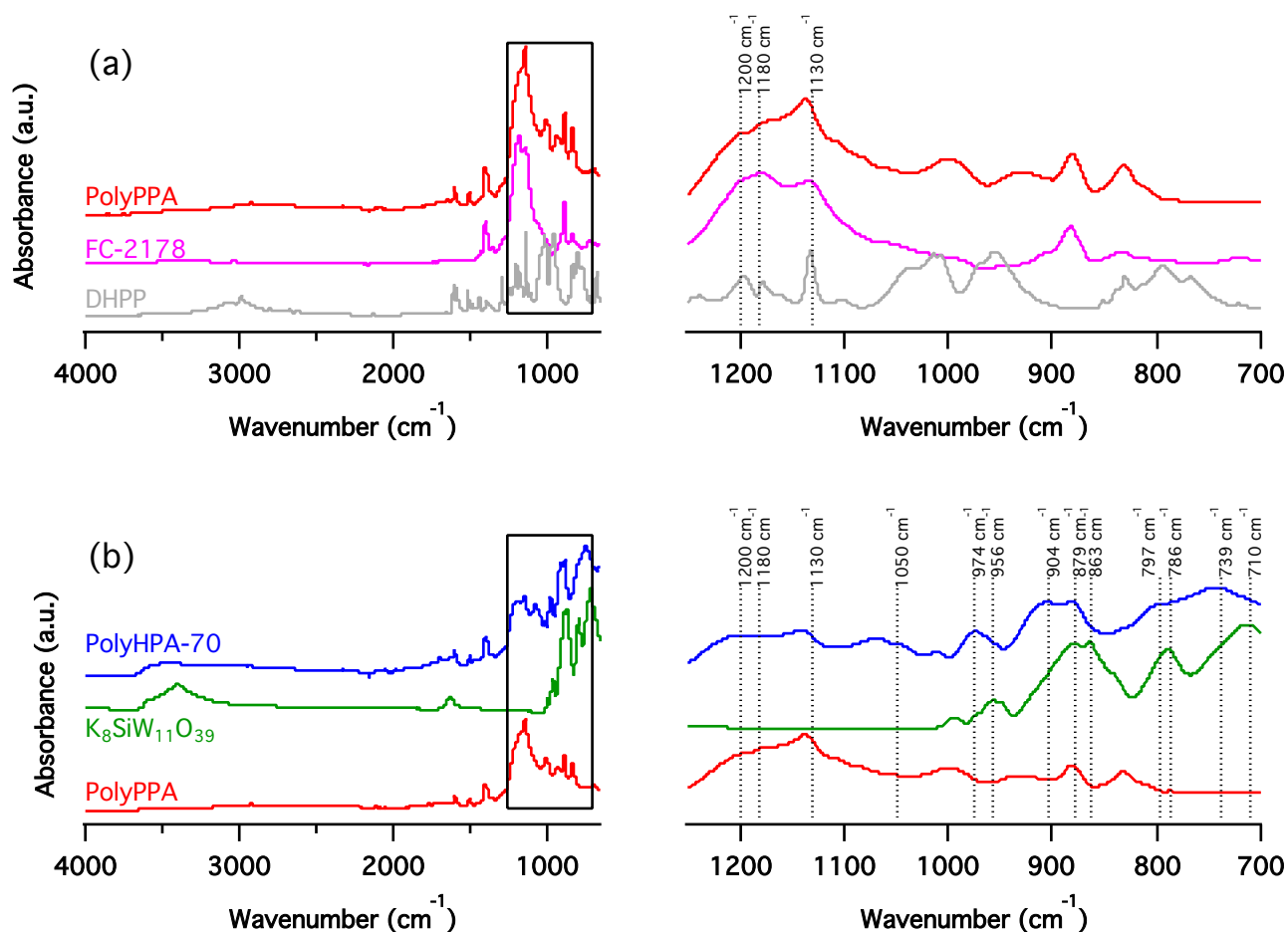


Figure S1: (a) IR data of the reactants and products for the attachment of phenol phosphonic acid side chains to FC-2178 (step 1 and 2 in scheme 1) with an expanded view of the boxed area displayed to the right (b) IR data of the reactants and product for the HSiW11 attachment to PolyPPA with an expanded view of the boxed area displayed to the left

More thorough analysis of these bands indicates a shift to higher wavenumbers after the attachment, as expected from the aforementioned work with attaching small, organic molecules. Additionally, a peak at 1050 cm^{-1} is present in the product and neither of the reactants. Previous studies have concluded that in phenylphosphonic acid $\nu_{\text{as}}(\text{P-OH})$ is located at 1017 cm^{-1} and for $[\gamma\text{-SiW}_{10}\text{O}_{36}(\text{C}_4\text{H}_5\text{PO})_2]^{-4}$ $\nu_{\text{as}}(\text{P-OW})$ is located at 1050 cm^{-1} .^{3,4} A list of assignments are presented in Table

S1. While the IR data provides compelling evidence that the synthesis has occurred as expected, NMR was used to corroborate the covalent attachment of HSiW.

Table S1: Assignments of FTIR bands in cm^{-1} according to previous studies ^{4,5,2}

	$\text{K}_8\text{SiW}_{11}\text{O}_{39}$	PolyHPA
$\nu_{\text{as}}(\text{P-O})$	-	1050
$\nu_{\text{as}}(\text{Si-O}_a)$	956	974
$\nu_{\text{as}}(\text{W=O}_{\text{ter}})$	879	904
	863	879
$\nu_{\text{as}}(\text{W-O}_e\text{-W})$	768	797
$\nu_{\text{as}}(\text{W-O}_c\text{-W})$	710	739

Further evidence for the validity of the synthetic scheme was provided by ^1H NMR (Figure S2a). First in the DHPP, the aromatic protons are located at 6.9 and 7.5 ppm and the $-\text{CH}_2-$ and $-\text{CH}_3$ chemical shifts are at 3.9 and 1.2 ppm, respectively. The $-\text{CH}_2-$ groups in the FC-2178 are located between 2.7 and 3.3 ppm. When the DHPP is attached to the polymer, the product contains the same $-\text{CH}_2-$ signals from the FC-2178 in addition to the aromatic signals and the signals at 3.9 and 1.2 ppm. Next, the hydrolysis reaction is performed on the PolyPPE and the phosphonate ester $-\text{CH}_2-$ and $-\text{CH}_3$ chemical signatures are eliminated, as expected, and a new signal exists at 6.5 ppm and is assigned to the $-\text{OH}$ bonds.

The ^{19}F NMR (Figure S2b) indicates that when adding the sidechain, an additional signal at -55 ppm appears which is consistent with other studies on PVDF-HFP functionalization.⁶ Perhaps the most compelling evidence for the functionalization of the polymer comes from ^{31}P NMR (Figure S2c and Figure S2d). First, when the DHPP is attached to the polymer there is a change in chemical shift (21 \rightarrow 17.5 ppm) and the signal becomes more broad and complex, one indication that the P nuclei are associated with a polymer. At this point, some unattached DHPP is still present (sharp signal at 21 ppm), but after the hydrolysis step, the sharp signal at 21 ppm vanished and the only peak is at 12 ppm (the expected shift for PolyPPA). The final HSiW11 attached film is cross-linked and not soluble in NMR solvents; therefore, liquid ^{31}P NMR is not possible on the final film. To probe the chemical nature of the final material ^{31}P CP/MAS NMR was performed on both PolyPPA and PolyHPA-70. The chemical shift of PolyPPA is different in the solid phase than it is in the liquid NMR likely due to the water content and solvation and is shown for comparison to the PolyHPA-70 (Figure S2d). Using a Gaussian fit to model the spectra, four chemical shifts are identified (23, 20.5, 15.1, and 9.5 ppm). The signal at 20.5 ppm is residual phenol phosphonic acid. The three remaining signals are assigned to HSiW11 with one phosphorous attachment (23 ppm), HSiW11 with two phosphorous attachments (15.1 ppm), and a phosphorous anhydride (9.5 ppm).⁷ The phosphorous anhydride is presumably formed between two unreacted phenol phosphonic acid side chains at elevated temperatures through the loss of a water molecule.

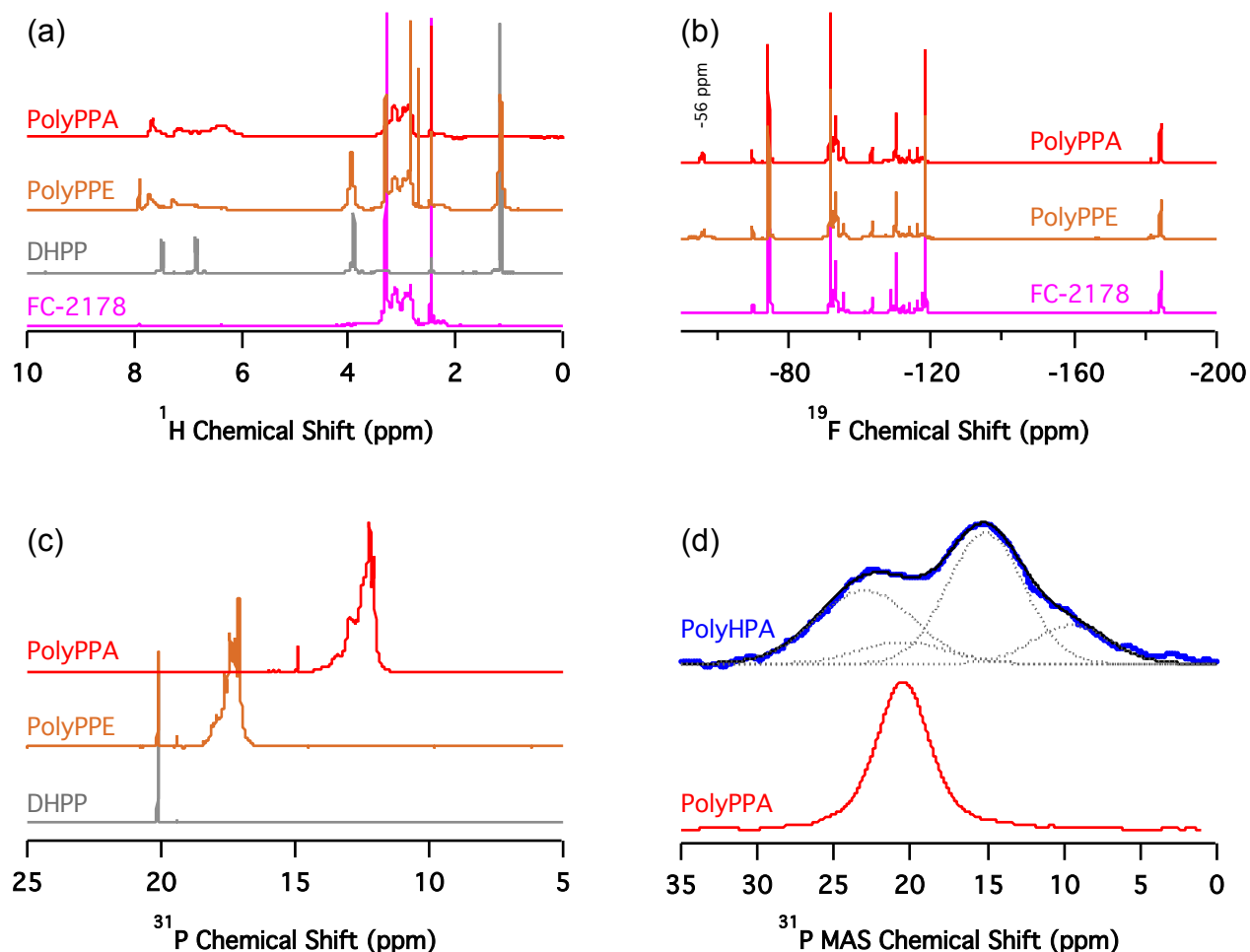


Figure S2: (a) ^1H NMR for PolyPPA, PolyPPE, DHPP, and FC-2178 where the remaining solvent signals are labelled * (b) ^{19}F NMR data for PolyPPA, PolyPPE, and FC-2178 (c) ^{31}P NMR of DHPP, PolyPPE, and PolyPPA (d) $^1\text{H} \rightarrow ^{31}\text{P}$ CP/MAS NMR of PolyPPA and PolyHPA-70 where the PolyHPA-70 spectra is modelled using 4 different Gaussian functions

IEC calculation using TGA:

Due to instability of HPAs at high pH, the IEC was calculated using data from TGA. The TGA data below in Figure S3, which shows that at 800 °C in air nearly all of the PolyPPA has volatilized < 4 % remaining. Conversely, the PolyHPA-70 has a residual normalized mass of 56 %. The calculation for the theoretical IEC assumes that each silicotungstic acid moiety has 13 hydrating waters at room temperature and humidity, a common hydration state of the monolacunary silicotungstic acid.^{8,9} Assuming that in air at 800 °C each element is in its most oxidized form would result in 11 WO_3 and 1 SiO_2 for each HSiW_{11} , which has been previously observed for $\alpha\text{-H}_4\text{SiW}_{12}\text{O}_{40}$ using x-ray diffraction and FTIR.¹⁰

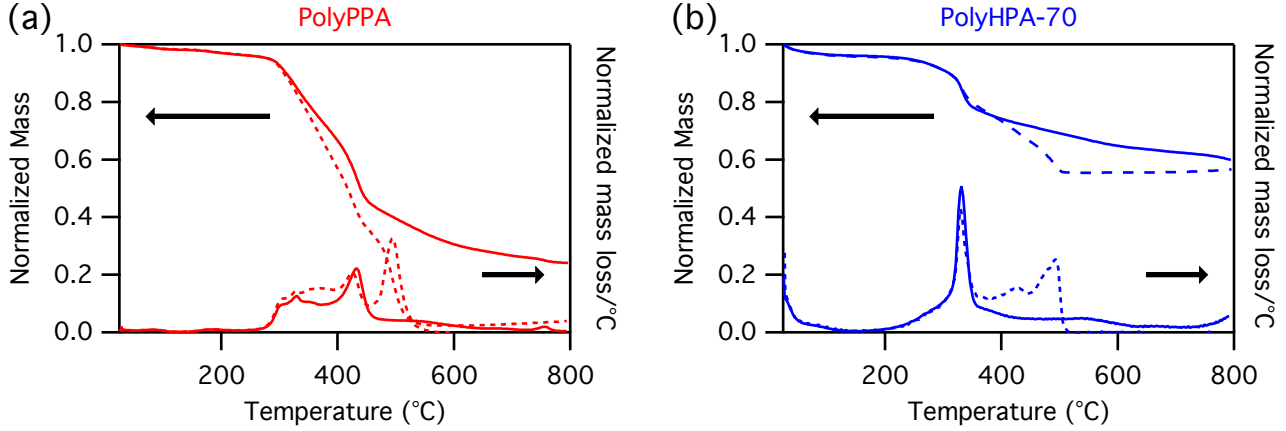


Figure S3: TGA data in N₂ (solid lines) and air (dashed lines) for (a) PolyPPA residue in air at 700°C is 2% (b) PolyHPA-70 residue in air at 800°C is 56%

Calculating the actual IEC from the TGA residue:

$$\left(\frac{1 \text{ mol SiW}_{11}\text{O}_{39}}{11 \text{ mol WO}_3 + 1 \text{ mol SiO}_2} \right) * \left(\frac{4 \text{ mol H}^+}{1 \text{ mol SiW}_{11}\text{O}_{39}} \right) * \left(\frac{11 \text{ mol WO}_3 + 1 \text{ mol SiO}_2}{11 * 231.8 + 1 * 60.8 \text{ g residue}} \right) = \frac{0.0015 \text{ mol H}^+}{\text{g residue}}$$

$$\left(\frac{0.56 \text{ g residue}}{1 \text{ g Polymer}} \right) * \left(\frac{0.0015 \text{ mol H}^+}{\text{g residue}} \right) * \left(\frac{1000 \text{ mmol H}^+}{1 \text{ mol H}^+} \right) = 0.86 \frac{\text{mmol H}^+}{\text{g Polymer}}$$

Calculating the theoretical residue from adding 70 wt% a-K₈SiW₁₁O₃₉•13(H₂O) and 30 wt% PolyPPA:

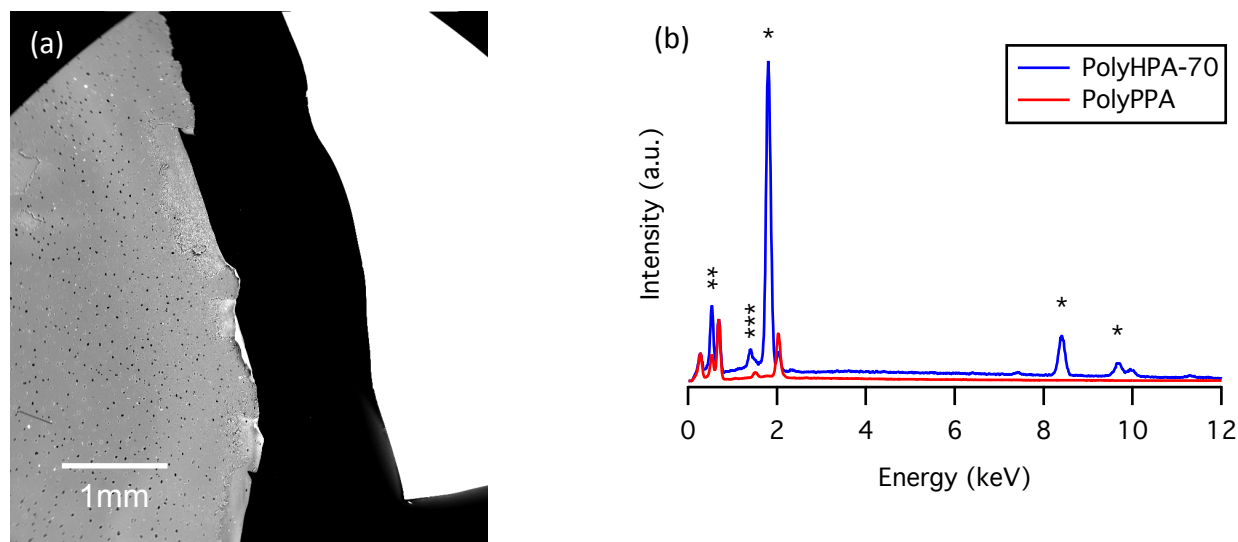
$$\left(\frac{0.70 \text{ g K}_8\text{SiW}_{11}\text{O}_{39} \cdot 13\text{H}_2\text{O}}{1 \text{ g PolyHPA}} \right) * \left(\frac{1 \text{ mol K}_8\text{SiW}_{11}\text{O}_{39} \cdot 13\text{H}_2\text{O}}{3221 \text{ g K}_8\text{SiW}_{11}\text{O}_{39} \cdot 13\text{H}_2\text{O}} \right) * \left(\frac{11 \text{ mol W}}{1 \text{ mol K}_8\text{SiW}_{11}\text{O}_{39} \cdot 13\text{H}_2\text{O}} \right)$$

$$= \frac{0.00239 \text{ mol W}}{\text{g PolyHPA}}$$

$$\left(\frac{0.00239 \text{ mol W}}{\text{g PolyHPA}} \right) * \left(\frac{1 \text{ mol WO}_3}{1 \text{ mol W}} \right) * \left(\frac{231.8 \text{ g WO}_3}{1 \text{ mol WO}_3} \right) = \frac{0.554 \text{ g WO}_3}{\text{g PolyHPA}} = 0.83 \frac{\text{mmol H}^+}{\text{g Polymer}}$$

If we add 70wt% a-K₈SiW₁₁O₃₉•13(H₂O), we would expect to have 55.4% residue at 800°C if all is converted to WO₃ which matches very well with the 56% observed experimentally. The discrepancy may be due to unvolatilized PolyPPA residues or experimental error.

An additional technique that was attempted to use for determination of the loading of HSiW11 was EDS, see Figure S4. First, the SEM figure shows that the PolyHPA-70 membrane is much brighter than the PolyPPA membrane in the backscatter micrograph, one indication that we do have a large amount of heavy elements in the washed film. Additional evidence comes from the W signature in EDS, which is very prominent in the washed PolyHPA-70 film. While quantitative values are given, they are unrealistic and unreliable and should only be considered as semi-quantitative evidence that a large amount of W is present in the film after HSiW11 attachment and subsequent acid and water washes.



(c)

	PolyPPA		PolyHPA-70	
	wt%	at%	wt%	at%
C	34.7 ± 0.5	46.5 ± 0.7	10.2 ± 1.3	28.7 ± 0.4
O	17.5 ± 0.5	17.6 ± 0.5	13.9 ± 3.0	29.0 ± 2.7
F	33.9 ± 1.0	28.7 ± 0.8	8.7 ± 1.8	15.4 ± 1.4
Al	1.4 ± 0.1	0.8 ± 0.1	0.3 ± 0.1	0.4 ± 0.1
Si	0.2 ± 0.1	0.1 ± 0.1	12.6 ± 0.4	15.2 ± 2.1
P	11.9 ± 0.3	6.2 ± 0.1	1.3 ± 0.0	1.5 ± 0.2
W	0.5 ± 0.2	0.0 ± 0.0	52.9 ± 5.6	9.8 ± 2.0

Figure S4: (a) SEM of PolyPPA (left) and PolyHPA-70 (right) (b) EDS data comparing PolyPPA and PolyHPA-70 to each other where the PolyHPA data was normalized using C Ka and F Ka from PolyPPA. Discrepancies are the result of added W (*) and O (**). The Al peak (***) is also different. (c) Table with calculated values for abundance of the difference elements

Annealing Process:

Using DSC and SAXS, the thermal behaviour of the unannealed PolyHPA-70 was investigated, see Figure S5. Contrasting the DSC data for PolyPPA (Figure S5a) with the DSC data for PolyHPA-70 (Figure S5b) one key difference exists; an exothermic event between 120 and 200 °C for the PolyHPA-70. This event was thought to be either an irreversible change in morphology (crystallization) or a chemical reaction. To further probe this event, an *in-situ* SAXS experiment was performed (Figure S5c). An unannealed PolyHPA-70 film was loaded in an environmental chamber and dynamic SAXS data was collected as the temperature was ramped up to 160°C and then held for 5 min before cooling to room temperature. The SAXS pattern showed the 6.5 nm clustering the entire time and it is concluded that the exothermic event observed in DSC was not the formation of these clusters or any other morphology change. This exothermic event is therefore assigned to an exothermic reaction. The two potential reactions are additional HSiW11 attachment to PolyPPA side chains or two PolyPPA side chains reacting with each other to form a phosphorous anhydride. ³¹P NMR evidence for a change in the P environments between the polymer solution that was cast and the final, annealed film can be seen in Figure S5d. For fair comparison, the PolyPPA signal has been set to 12.5 ppm as an internal standard to allow

comparison between the liquid and solid-state NMR data. The relative abundance of the phenol phosphonic acid signal is lower after the high pressure annealing step, indicative of its involvement in a reaction. This reaction is assigned to result from contributions from both additional HSiW11 attachment and formation of an anhydride through the loss of water resulting in a new signal more downfield from all of the other ^{31}P chemical shifts.

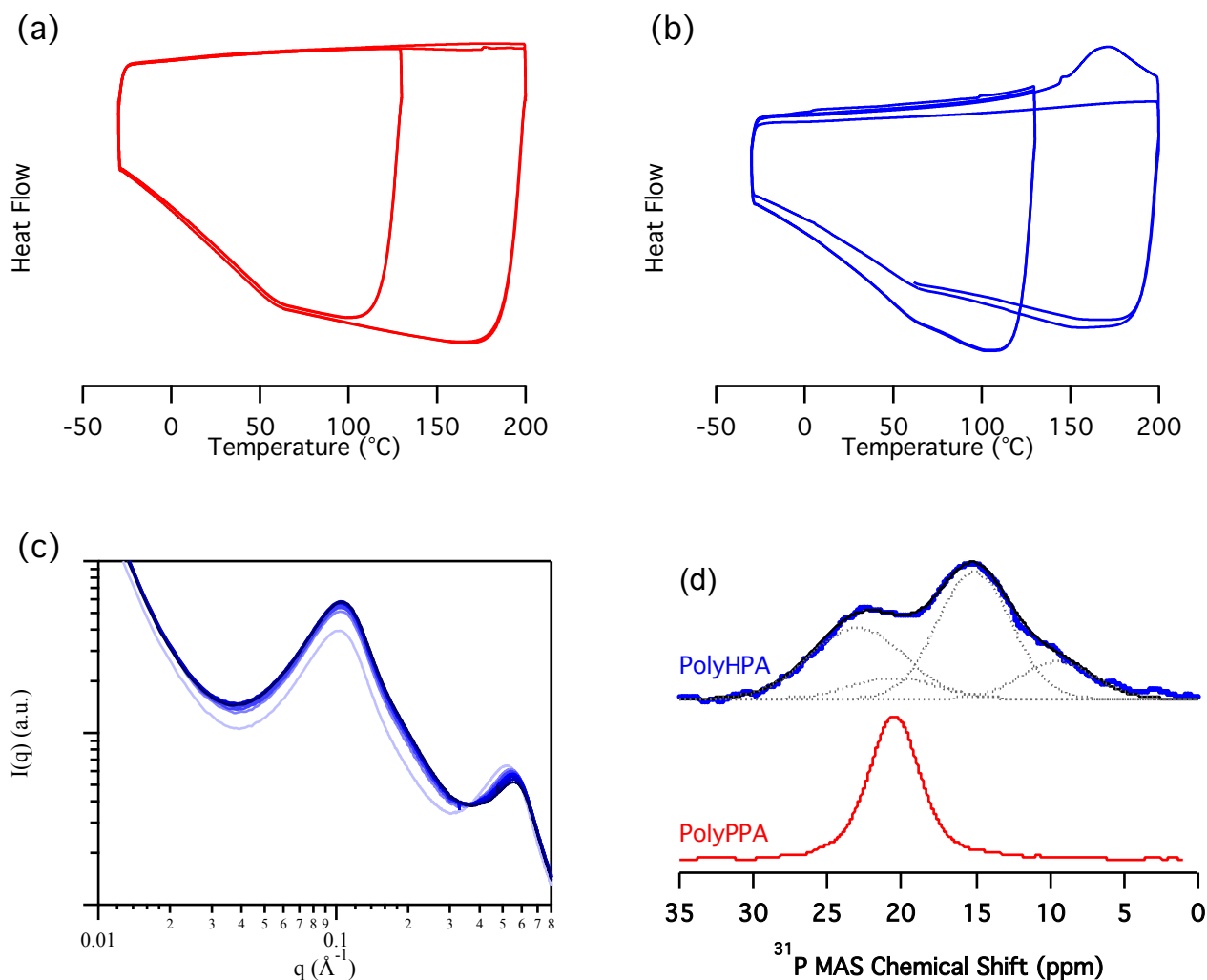


Figure S5 (a) DSC of PolyPPA (b) PolyHPA (c) SAXS data for an in-situ annealing study where the film was heated from room temperature to 160°C then held for 5 minutes. Notice the clustering is present through out the experiment.

Once these films were made, the initial interest was mechanical and chemical stability. Two films were tested in the chemical stability test and one was tested in the mechanical stability test. The fuel cell that was tested in the mechanical stability test was fabricated using a CCM method and while it passed the mechanical AST, the fuel cell performance was very poor. The rest of the PolyHPA fuel cells were made using commercial GDEs and showed much greater performance, see Figure 4 in the main text. The end of life performance for the fuel cell that passed the mechanical AST can be seen in Figure S6.

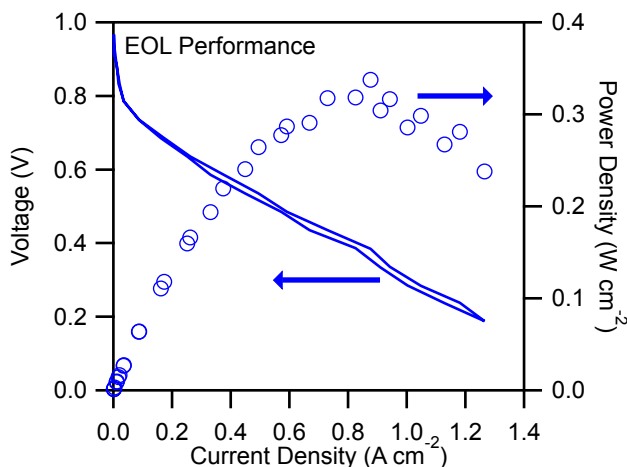


Figure S6: Data from Mechanical AST that was conducted on an 80 μm film with each cycle consisting of 30 second dry / 30 second wet N_2 flow the polarization data collected after 22,500 cycles at 80°C/100 %RH

The proton conductivity of PolyHPA-75 under various humidities can be seen in Figure S7. To study the stability of this material in warm water, a film was soaked for 16 h at 80 °C and the conductivity was measured afterwards. The loss in conductivity is greater at low humidities.

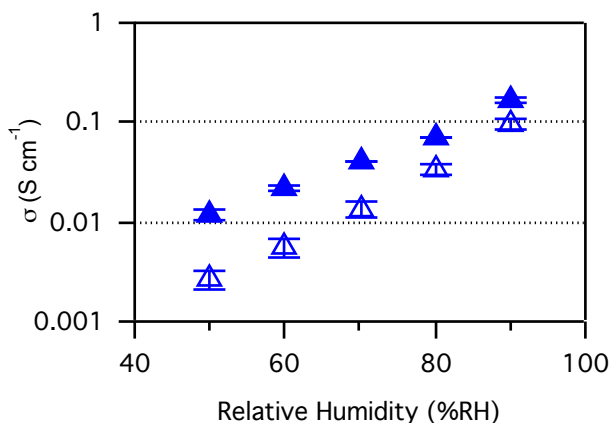


Figure S7: *Ex-situ* conductivity data of PolyHPA-75 at 80 °C under various humidities (▲) film washed in room temperature water (△) film washed in 80 °C water for 16 h

References:

1. H. W. Starkweather, R. C. Ferguson, D. B. Chase and J. M. Minor, *Macromolecules*, 1985, **18**, 1684-1686.
2. C. Rocchiccioli-Deltcheff, M. Fournier, R. Franck and R. Thouvenot, *Inorganic Chemistry*, 1983, **22**, 207-216.
3. W. Förner and H. M. Badawi, *Journal of Structural Chemistry*, 2011, **52**, 471-479.
4. C. R. Mayer, P. Herson and R. Thouvenot, *Inorganic Chemistry*, 1999, **38**, 6152-6158.
5. G. S. Kim, K. S. Hagen and C. L. Hill, *Inorganic Chemistry*, 1992, **31**, 5316-5324.
6. A. Taguet, B. Ameduri and B. Boutevin, *Journal of Polymer Science Part a-Polymer Chemistry*, 2006, **44**, 1855-1868.

7. S. Kobayashi, T. Chow, H. Kawabata and T. Saegusa, *Polymer Bulletin*, 1986, **16**, 269–276.
8. K. Y. Matsumoto and Y. Sasaki, *Bulletin of the Chemical Society of Japan*, 1976, **49**, 156-158.
9. J.-Y. Niu, J.-W. Zhao and J.-P. Wang, *Inorganic Chemistry Communications*, 2004, **7**, 876-879.
10. D.-J. Wang, Z.-D. Fang and X.-H. Wei, *Chinese Journal of Chemistry*, 2005, **23**, 1600-1606.